American Journal of Pathology, Vol. 161, No. 6, December 2002

Targeted Inactivation of the Mouse Guanylin Gene Results in Altered Dynamics of Colonic Epithelial Proliferation

Kris A. Steinbrecher,*† Steve A. Wowk,* Jeffrey A. Rudolph,* David P. Witte,‡ and Mitchell B. Cohen*†

From the Division of Pediatric Gastroenterology, Hepatology and Nutrition, the Graduate Program in Molecular and Developmental Biology,† and the Division of Pediatric Pathology,‡ Children's Hospital Research Foundation, Children's Hospital Medical Center and University of Cincinnati, Cincinnati, Ohio*

Heat-stable enterotoxin (STa), elaborated by enterotoxigenic *Echerichia coli*, is a worldwide cause of secretory diarrhea in infants and travelers. Both STa and guanylin, a peptide structurally similar to STa, increase intracellular cGMP levels after binding to the same intestinal receptor, guanylate cyclase C (GC-C). Distinct from its role as an intestinal secretagogue, guanylin may also have a role in intestinal proliferation, as guanylin expression is lost in intestinal adenomas. To determine the function of guanylin in intestinal epithelia, guanylin null mice were generated using a Cre/*loxP*-based targeting vector. Guanylin null mice grew normally, were fertile and showed no signs of malabsorption. However, the levels of cGMP in colonic mucosa of guanylin null mice were significantly reduced. The colonic epithelial cell migration rate was increased and increased numbers of colonocytes expressing proliferating cell nuclear antigen (PCNA) were present in crypts of guanylin null mice as well. The apoptotic index was similar in guanylin null mice and littermate controls. We conclude from these studies that loss of guanylin results in increased proliferation of colonic epithelia. We speculate that the increase in colonocyte number is related to decreased levels of cGMP and that this increase in proliferation plays a role in susceptibility to intestinal adenoma formation and/or progression. *(Am J Pathol 2002, 161:2169–2178)*

Ion flow across epithelial cell membranes is tightly controlled by various factors, including hormones and the enteric nervous system. Dysregulation of this system by bacterial pathogens is the basis for many secretory diarrheal diseases. Enterotoxigenic *Escherichia coli* that elaborate heat-stable enterotoxin (STa) are a worldwide cause of secretory diarrhea, especially in infants and travelers.[1]

The low-molecular-weight peptide guanylin is highly homologous to STa and is secreted from the epithelial cell layer of the small and large intestine.[2–4] Once elaborated into the intestinal lumen, guanylin, another similar mammalian peptide, uroguanylin, and STa can all bind to the receptor guanylate cyclase C (GC-C), located on the enterocyte brush border membrane.[5–7] Ligand binding to GC-C initiates a signal transduction cascade that culminates in activation of the cystic fibrosis transmembrane conductance regulator (CFTR).[8,9] In this system, STa acts as a superagonist that results in secretory diarrhea. Similarity in structure between guanylin and STa led to the hypothesis that guanylin contributes to regulation of gastrointestinal fluid homeostasis. However, distinct from its role as an intestinal secretagogue, guanylin may also have a role in intestinal proliferation. For example, we have previously shown that guanylin expression is lost in mouse and human intestinal adenomas.[10,11]

To determine the effect of loss of guanylin activity in the whole animal, we inactivated the mouse guanylin gene using homologous recombination. We used the Cre/*loxP* system to target the mouse guanylin gene in a manner that allowed for removal of the targeting selection cassette and minimal alteration of the sequence surrounding the guanylin allele.[12] We demonstrate that mice lacking guanylin develop normally, are fertile, and display no evidence of intestinal obstruction or obvious loss in intestinal absorptive capacity. However, we demonstrate that levels of cGMP are lower in the colonic epithelia of guanylin null mice. Furthermore, we show that the amount of apoptosis in intestinal epithelia is unchanged but the rate of proliferation of colonic epithelia in these mice is significantly increased.

Supported by grant DK 47318 from the National Institutes of Health.

Accepted for publication September 9, 2002.

Address reprint requests to Mitchell B. Cohen, M.D., Division of Pediatric Gastroenterology, Hepatology, and Nutrition, Cincinnati Children's Hospital Medical Center, MLC 2010, 3333 Burnet Avenue, Cincinnati, OH 45229. E-mail: mitchell.cohen@chmcc.org.

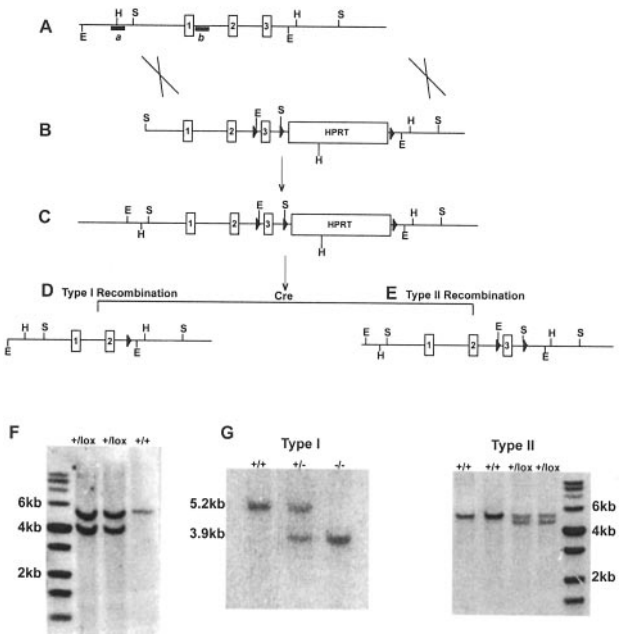

Figure 1. Gene targeting of the mouse guanylin locus. **A:** The mouse guanylin gene is composed of three exons and spans ~1.7 kb with the physiologically active ligand portion of the gene encoded by exon 3. Indicated are the restriction sites of the wild-type allele and probes (*a,b*) used to visualize these bands during Southern analysis. **B:** A Cre/*loxP*-based replacement vector that consisted of three *loxP* sites flanking the third exon and an HPRT selection cassette, as well as outer regions of homologous sequence was used to target the mouse guanylin gene. **C:** Recombination results in the targeted guanylin allele. **D** and **E:** Subsequent expression of the Cre recombinase eliminates some or all of the floxed sequence, yielding either Type I or Type II deletions. **F:** Identification of the initial targeted allele found in ES cell clones used *Eco*RI (5.4 kb and 4.1 kb) and *Hind* III with probe (*A,*) which is comprised of sequence outside the targeting construct. **G:** Following rearrangement of the allele by the Cre enzyme, we identified Type I and II deletions using *Sac*I digests and internal probe (*B*). PCR screening was used to confirm Southern analysis results. E, *Eco*RI; H, *HinD* III; S, *Sac*I.

Materials and Methods

Construction of the Guanylin Allele Targeting Vector and Production of Guanylin Null Mice

The targeting construct contained the third exon of the guanylin gene, which encodes for the active guanylin peptide, as well as an hypoxanthine-guanine phosphoribosyl transferase (HPRT) selection cassette flanked by *loxP* sites (Figure 1). Cloning of the complete mouse guanylin gene and surrounding sequence was described previously.[13] A *loxP*-flanked, or floxed, HPRT selection cassette and Cre recombinase expression plasmid used in these studies were generously provided by Dr. Joanna Groden of the University of Cincinnati. All bacterial transformations and preparations were performed according to standard practices with recombination-deficient STBL2 competent *E. coli* cells (Life Technologies, Gaithersburg, MD). Construction of the guanylin targeting vector began by cloning a single *loxP* site into the second intron of guanylin. A 4.5-kb fragment (− 1886 to + 2714; numbering based on Reference 32) that encompassed the entire guanylin gene and the intronic *loxP* was placed just 5[prime] of the floxed HPRT cassette. Polymerase chain reaction (PCR) was performed using *Pfu* DNA polymerase to amplify a 4.0-kb region (+2714 to + 6653) downstream of exon 3 of the guanylin gene region. This PCR fragment was then cloned into the 3[prime] end of the floxed HPRT cassette. This vector, pGEM(1E12), containing the floxed third exon of guanylin and a floxed HPRT cassette, was used to target the mouse guanylin gene locus (Figure 1). Before this, the construct was sequenced (University of Cincinnati Sequencing Core) at all ligation junctions and *loxP* sites to ensure base sequence fidelity and correct orientation of *loxP* sequence.

The University of Cincinnati Transgenic Core Facility performed all embryonic stem (ES) cell targeting and blastocyst injection procedures based on our genotyping of clones as detailed below. The targeting vector pGEM (1E12) was linearized and electroporated into 129/SV strain E14 ES cells. All genotyping of both ES cells and mice was performed using Southern analysis or PCR according to standard protocols. Of 220 ES cell clones screened by Southern analysis, 15 correctly recombined clones were identified. Southern analysis was performed using *Eco*RI, *Xba*I, and *Hin*d III restriction enzyme digests with three probes that hybridize to regions inclusive or exclusive of the original targeting vector sequence. Restriction sites are shown in Figure 1, as are two probes used in Southern analysis. Following electroporation with a Cre recombinase expression plasmid, PCR screening and Southern analysis was used to identify ES cells containing either Type I (total recombination between outer *loxP* sites, Figure 1D) or Type II recombinations (recombination between the *loxP* sites that flank the HPRT cassette, Figure 1E). The vast majority of clones were Type I deletions but several also contained the Type II, floxed third exon allele. Clones from both the Type I and II deletion ES cells were injected into C57BL/6-derived blastocysts and implanted into pseudopregnant females.

All mice used in these studies were cared for under guidelines defined by the University of Cincinnati or the Children's Hospital Medical Center Institutional Animal Care and Use Committee. Mice had access to food and water and were housed in a temperature, humidity, and light-cycle controlled pathogen-free, micro-isolation facility. The studies described here were performed on mice bred 3 to 4 generations into the Balb/C strain and littermate mice were used as control animals.

Northern Analysis

Animals were sacrificed by CO_2 asphyxiation; this was performed during a 2-hour window to avoid differences in circadian expression of guanylin and uroguanylin. For protein and mRNA studies, the intestine was flushed with cold saline, separated into segments, and stored at − 80°C. Intestinal segments were defined as follows: proximal jejunum (proximal third of the small intestine); ileum (distal third of the small intestine); cecum; proximal colon (proximal 40% of colon); and distal colon (distal 60% of the colon). Frozen tissue was pulverized in chilled mortars and pestles and RNA was extracted using Trizol reagent (Gibco BRL, Gaithersburg, MD) as described previously.[14] Portions of the guanylin, uroguanylin, guanylate cyclase-C, down-regulated in adenoma (DRA), so-

dium hydrogen exchanger 3 (NHE3), and aquaporin 4 and 8 cDNAs were radiolabeled with [α-^{32}P] (DuPont-NEN, Boston, MA) using the Random Primer Labeling system (Roche Molecular Biochemicals, Indianapolis, IN) as described previously.[15,16] Blots were visualized and quantitated using a Molecular Dynamics PhosphorImager system (Molecular Dynamics, Sunnyvale, CA).

Western Analysis

Animals were sacrificed and tissues collected as described above. Tissue was homogenized and processed as described previously.[14] Membranes were immunoblotted using a 1:1000 dilution of antisera that recognizes proguanylin (antibody 2538) and prouroguanylin (antibody 6910).[14] These antibodies were generously provided by Dr. Michael Goy of the University of North Carolina and have been validated and described previously.[17,18] Following incubation with a horseradish peroxidase-conjugated secondary antibody, signal was visualized on Kodak X-OMAT AR film using a commercially available chemiluminescent kit (NEN Life Science Products, Boston, MA). As a control for loading, blots were reevaluated with an actin probe (gift of J.L. Lessard, Children's Hospital Research Foundation, Cincinnati, OH).

Histology

Guanylin heterozygous and null animal littermates were sacrificed and tissues collected as above except that tissue was initially placed in 10% neutral-buffered formalin. Intestinal tissue was cut longitudinally on foam biopsy sponges and fixed as flat sheets. After fixing for ~18 hours in formalin, samples were then removed and dehydrated through an increasing ethanol series over an 6-hour period, cleared in the xylene substitute Hemo-D (Fisher Scientific, Pittsburgh, PA) for 2 hours, and infiltrated with two changes of paraffin (Paraplast X-Tra Tissue Embedding media, Fisher Scientific) for 1 hour each. Tissue was then mounted in paraffin blocks and sectioned at 5-μm thickness for subsequent analysis.

Initial characterization of both guanylin heterozygous and null mouse intestinal sections was performed using Harris' hematoxylin and eosin staining according to standard protocols. To identify goblet cells, we used periodic acid-Schiff (PAS) reagents to stain the mucin stores that are found in these cells. A commercially available PAS staining system (Sigma Diagnostics, St. Louis, MO) was used according to the manufacturer's protocol.

cGMP Measurements

Ileum and colon were dissected from both wild-type and guanylin null mice. These segments were flushed with phosphate-buffered saline and laid flat using a lengthwise incision. A glass slide was used to scrape the mucosal surface of these segments, and the scrapings were immediately placed in liquid nitrogen. The tissue was homogenized in 6% trichloroacetic acid to give a 10% w/v homogenate. The homogenate was washed five times with four volumes of water-saturated diethyl ether. These samples were then dried down under nitrogen for 30 minutes, and resuspended in 0.05 mol/L sodium acetate, pH 6.2. cGMP was then measured in a validated radioimmunoassay and cGMP extractions were normalized per gram of tissue wet weight.[19]

Guanylate Cyclase Assay

Two centimeters of terminal ileum and proximal colon were dissected from both wild-type and guanylin null mice, flushed with phosphate buffered saline, and transected longitudinally. Each segment was divided into equal pieces and submerged in 500 μmol/L 3-isobutyl-1-methylxanthine (IBMX; phosphodiesterase inhibitor) in Hanks' buffered salt solution (HBSS), pH 7.0, for 15 minutes. The explants were removed and placed in IBMX/HBSS in the presence or absence of 5 μmol/L STa and incubated for a further 15 minutes at 37°C. The explant was removed, homogenized in 6% trichloroacetic acid, and cGMP was extracted as described above. cGMP levels were measured by radioimmunoassay. Duplicate segments from each mouse were analyzed for basal activity and STa-stimulated cGMP accumulation. The guanylyl cyclase activity was measured as femtomoles cGMP produced per gram of tissue wet weight per minute incubation at 37°C.

Crypt Depth

Crypt depth, used as an estimate of proliferation and apoptosis rates in colonic epithelia,[20,21] was measured in proximal and distal colon of heterozygous and null mice as follows. Paraffin-embedded tissue was sectioned at 5.0-μm thickness and stained with hematoxylin and eosin as above. Crypts were measured using image analysis software (NIH Image 1.62, National Institutes of Health, Bethesda, MD) that had been calibrated with a micrometer slide image. The observer was blinded to genotype as all images were captured and measurements were performed. Criteria for selecting which crypts to measure included a clearly seen and continuous cell column on each side of the crypt and a completely visible crypt lumen and opening. Many crypts, from multiple sections prepared from 4 to 5 animals per group were measured to evaluate a total of 40 to 50 crypts per group.

Epithelial Cell Proliferation

Bromo-deoxyuridine (BrdU) incorporation was used as a marker to estimate epithelial cell migration rate, and therefore proliferation, in ileum and distal colon of guanylin heterozygous and null mice. BrdU was injected intraperitoneally (150 μg BrdU in phosphate-buffered saline per gram body weight) and mice were sacrificed at 1 hour, 24 hours, or 48 hours. Intestinal segments were fixed and embedded in paraffin as described above. Sections were processed as per the manufacturer's protocol for BrdU immunohistochemical staining (BrdU Staining kit, Zymed, South San Francisco, CA). Migration

distance was measured as follows. Images were digitally captured at × 200. In ileum, the distance from the distal-most Paneth cell to the farthest BrdU-positive cell was determined using NIH Image 1.62. In distal colon, the distance from the base of the crypt to the farthest migrated BrdU-positive cell was used.

Immunohistochemistry was used to determine the number of cells expressing proliferating cell nuclear antigen (PCNA) per crypt/villus unit in the ileum and per crypt in the distal colon. PCNA staining was performed on paraffin sections of guanylin heterozygous and guanylin null mouse ileum and distal colon according to manufacturer's protocol (PCNA Staining kit, Zymed). PCNA-positive cells in select, correctly oriented crypts were counted by an observer who was blinded to genotype.

Terminal Deoxynucleotidyl Transferase-Mediated dNTP-Biotin Nick End Labeling (TUNEL) Assay

Deparaffinized sections of mouse intestine were digested with proteinase K solution (Gibco BRL) (20 μg/ml) for 20 minutes at room temperature. Slides were rinsed in water and treated with 0.5% H_2O_2 for 10 minutes at room temperature. Test slides were incubated in terminal deoxytransferase (TdT) (Roche) (20 units in 100 μl of buffer with 1 μl of biotin-dUTP) (Roche) for 1 hour at 37°C. Slides were washed in water, incubated with strepavidin-horseradish peroxidase complex (Dako, Carpinteria, CA) for 30 minutes at room temperature, and detected with AEC (3-amino-9-ethylcarbazole) solution (Sigma) for 10 minutes. Positive control slides included sections predigested with deoxyribonuclease and negative control slides were run in parallel without TdT.

Statistical Analysis

All values are presented as mean ± SE. Unless otherwise stated, all comparisons are made between wild-type or heterozygous and null mice using the unpaired *t*-test. Differences were considered statistically significant at $P < 0.05$.

Results

Generation of Guanylin Null Mice

Following gene targeting of the mouse guanylin allele, mice were obtained that harbored the Type II deletion (Figure 1E), ie, the guanylin allele containing the floxed third exon but not the HPRT selection cassette. Unfortunately, no chimeric mice that produced Type I deletion (Figure 1D) agouti pups were obtained during these studies. To ablate the guanylin gene, we bred Type II deletion mice with cytomegalovirus (CMV)-Cre transgenic mice of the BALB/c genetic background strain. These transgenic mice express the Cre recombinase under the control of a human cytomegalovirus minimal promoter in all cells at the pre-implantation stage and beyond.[22] This allowed us to breed double transgenics, ie, animals with both the guanylin Type II allele and the CMV-Cre transgene. This generates a Type I deletion (Figure 1D) and this occurs before germline specification, resulting in animals that can pass this guanylin null allele to their offspring. We were able to breed mice that were homozygous guanylin null, suggesting the guanylin gene was not critical for development. Guanylin null mice grew normally to adulthood and were of similar weight as heterozygous controls. We continued breeding the guanylin null mice into the BALB/c strain and selected mice that did not contain the CMV-Cre transgene. This was the basis for the generation of the guanylin null animals used in the studies that are described here.

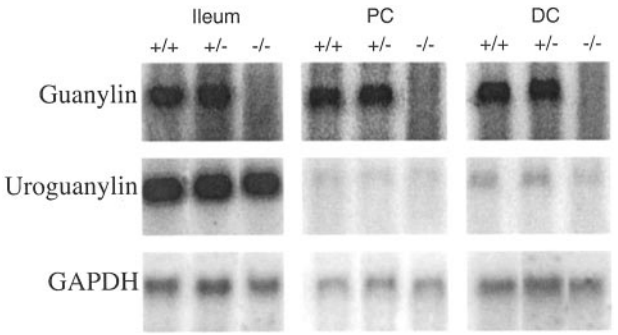

Figure 2. Northern analysis of guanylin wild-type, heterozygous, and null mice. **Top:** The entire guanylin cDNA was used as probe on Northern blots of ileum, proximal, and distal colon and no guanylin mRNA transcripts were seen in null mice. Guanylin mRNA levels were not diminished in heterozygous mice as compared to wild-types. **Middle:** Uroguanylin mRNA levels were not significantly altered in guanylin null mice when compared to wild-type or heterozygous animals. **Bottom:** GAPDH expression is shown. PC, proximal colon; DC, distal colon.

Northern and Western Analysis of Guanylin Null Mice

To confirm inactivation of the guanylin gene, we compared expression of guanylin mRNA and protein in guanylin null mice with that of guanylin wild-type and guanylin heterozygous mice. It was possible that the guanylin promoter was still active and that the first portion of the gene was still being transcribed as no direct changes were made to these regions during the initial targeting event or in subsequent Cre-mediated recombinations. To determine this, we hybridized a full-length guanylin cDNA probe to Northern blots of ileum, proximal colon, and distal colon RNA from wild-type, heterozygous, and null mice. No signal was found in guanylin null mice (Figure 2, top). This suggests that the guanylin promoter is inactive or that the partial guanylin transcripts that are produced are highly unstable. During our investigations, we noted no consistent difference between the level of guanylin mRNA expression in wild-type *versus* heterozygous littermates (Figure 2 and data not shown). Consequently, we used guanylin heterozygotes as littermate control animals in the experiments described here.

The guanylin and uroguanylin genes are located extremely close to each other at both mouse and human chromosomal loci (intragenic gap approximately 7 kb)

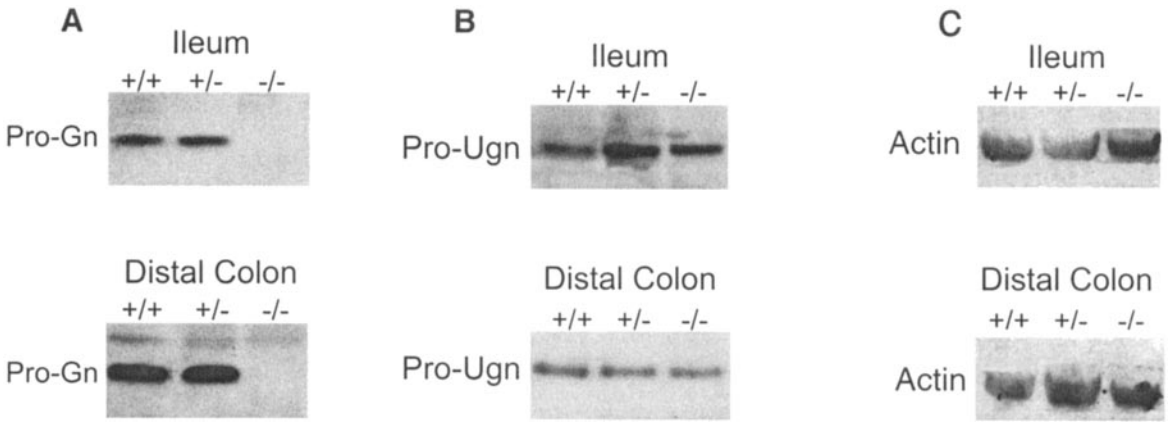

Figure 3. Western analysis of guanylin wild-type, heterozygous, and null mice. **A:** Guanylin prohormone was not found in tissue from the ileum and distal colon of guanylin null mice. **B:** Uroguanylin levels were unchanged in ileum and distal colon of guanylin null mice compared to wild-type or heterozygous animals. **C:** Actin levels are shown in ileum and distal colon as a control for loading. Pro-Gn, proguanylin; Pro-Ugn, prouroguanylin.

and their mRNA expression patterns and functional similarity suggests coordinate regulation in a manner that allows for the presence of a GC-C binding ligand in all regions of the intestinal tract.[13,16,23] Therefore, we determined the effect of loss of guanylin on uroguanylin levels. Uroguanylin mRNA levels are not affected by the manipulation of the mouse guanylin gene locus as expression is similar in both the small and large intestine of guanylin null mice when compared to that seen in guanylin wild-type and heterozygous animals and normalized by GAPDH expression (Figure 2, middle). GC-C mRNA levels were also unaffected (data not shown).

Western analysis of intestinal tissue from guanylin null mice was performed to confirm the loss of guanylin prohormone. We used antisera that was specific for the prohormone portion of the guanylin gene and expected to see the complete loss of proguanylin as suggested by the absence of even partial mRNA transcripts (Figure 2, top). Western blotting showed no traces of proguanylin found in ileum (Figure 3A, top) or in distal colon (Figure 3A, bottom) of guanylin null mice. Taken collectively, these Northern and Western data confirm the complete inactivation of the mouse guanylin gene.

We next determined that cellular levels of prouroguanylin were not affected by loss of proguanylin. Western analysis of small and large intestinal tissue homogenate demonstrated equal amounts of prouroguanylin peptide in null and heterozygous mice (Figure 3B). These data suggest that loss of the guanylin gene and activity does not affect levels of uroguanylin mRNA or prohormone in enterocytes, although further studies will be needed to determine whether levels of uroguanylin secretion into the intestine are altered in guanylin null mice.

We next sought to determine the mRNA levels of several genes known to be instrumental in fluid homeostasis in the mouse intestine. We found no difference in the mRNA levels of several ion and water channels such as the sodium-hydrogen exchanger 3 (NHE3), the chloride diarrhea anion exchanger (CLD), and aquaporins 4 and 8 (AQP4, AQP8) in guanylin null mice as compared to heterozygous littermate controls (data not shown).

Histological Examination of Guanylin Null Mice

We used hematoxylin and eosin staining to determine the small and large intestinal morphology of heterozygous and null animals. We noted no obvious abnormalities in crypt-villus structure in the ileum and in crypt morphology in the colon in nullizygous mice as compared to control.

Guanylin is expressed at especially high levels in goblet cells of the intestine.[18] We use periodic acid-Schiff (PAS) staining to identify goblet cells and determine whether loss of guanylin affected either goblet cell number or storage of mucin in these cells as judged by stain intensity. PAS reagents showed strong staining of goblet cell mucin in heterozygous and null mice and suggested no difference in goblet cell number or mucin storage (data not shown). Similarly, no difference was seen in apparent numbers of Paneth cells in the ileum of guanylin heterozygous and guanylin null mice (data not shown).

Uroguanylin expression is very robust in the small intestine and guanylin expression is highest in the large intestine of wild-type mice. Because it seems likely that these genes have similar functions, we speculated that the phenotype generated from the loss of the guanylin gene might be found in the large intestine due to compensatory actions of uroguanylin in the small intestine. Therefore the studies described here were designed to measure the effects of guanylin loss on the colon, with small intestinal segments often included as examples of tissues that are not devoid of a GC-C-binding peptide.

cGMP Levels in Intestinal Mucosa of Guanylin Null Mice

GC-C is the major transmembrane guanylate cyclase in the intestine and the only known endogenous ligands of GC-C are guanylin and uroguanylin. Loss of guanylin might be expected to result in diminished cGMP levels in regions of the intestine that do not have appreciable levels of uroguanylin. We determined cGMP content in mucosal scrapings from ileum and colon of wild-type and

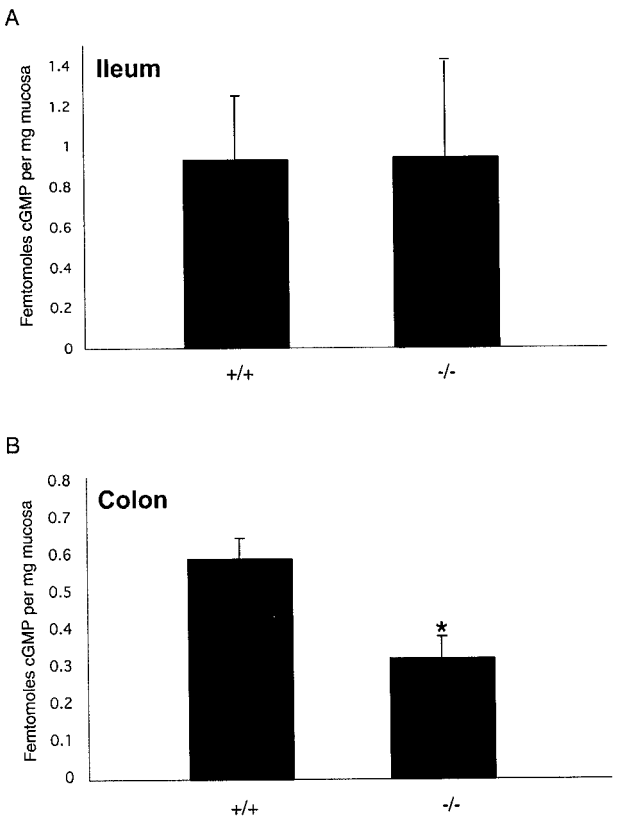

Figure 4. cGMP levels in epithelia of ileum and colon. **A:** Levels of cGMP in ileal epithelia of guanylin null mice were similar to that of wild-type littermates. **B:** Guanylin null mice have significantly less cGMP in colonic mucosa when compared to wild-type controls. Values are presented as mean ± SE. $n = 5$ mice per genotype; *, $P < 0.05$.

null mice by radioimmunoassay. The amount of cGMP in ileum of wild-type littermates and guanylin null mice was similar, although there was significant animal-to-animal variation (Figure 4A). Colonic cGMP, however, were markedly different in each genotype. cGMP levels in the colon were decreased considerably in guanylin null mice as compared to wild-type littermates (Figure 4B), suggesting the loss of this guanylate cyclase-activating peptide resulted in lowered basal levels of cGMP in the epithelia of the colon. To further characterize the guanylate cyclase pathway in these animals, we also measured the activity of GC-C in ileal and colonic explants. In the ileum ($n = 2$), cGMP levels increased 3.5-fold (range, 2.7 to 4.4) in wild-type animals and 2.5-fold (range, 2.2 to 2.7) in null mice on addition of STa. In the colon ($n = 2$), cGMP levels increased 1.5-fold (range, 1.4 to 1.5) in wild-type and 1.5-fold (range, 1.3 to 1.6) in null mice on addition of STa. Thus the decreased levels of cGMP in the colon are not due to diminished activity of GC-C.

Proliferation of Intestinal Epithelia in Guanylin Null Mice

cGMP signaling has been linked to control of proliferation in some cell types.[24–26] Therefore, we tested the hypothesis that loss of guanylin results in proliferative changes in the colon. A general measure of these parameters is the depth of the crypt glands as has been measured in the small intestine.[20,21] Alterations in the cellular division rate of intestinal epithelia result in increased or decreased crypt depth and, consequently, are reflected in crypt depth measurements. We adapted this technique for use in the colon and found significant increases in crypt depth in both the proximal and distal colon of guanylin null mice as compared to heterozygotes (Table 1). Increases in crypt depth in both proximal and distal colon were approximately 10%. Additional studies have determined that the number of epithelial cells per crypt in the distal colon is increased in the guanylin null mice when compared to heterozygous littermate controls (44.6 ± 1.4 cells *versus* 39.6 ± 1.5 cells; $n = 12$ to 20; $P = 0.01$). This increase, of approximately 10%, is consistent with the quantitative change in crypt depth.

Table 1. Crypt Depth in Proximal and Distal Colon of Guanylin Heterozygous and Null Mice

	Guanylin heterozygous (μm)	Guanylin null (μm)
Proximal colon	77.0 ± 2.5	83.4 ± 1.5*
Distal colon	138 ± 4.8	153 ± 3.0*

Crypt length was measured as detailed in Material and Methods. Within each group, a total of 40–50 crypts were measured. Only crypts with easily visible crypt cell columns and unobstructed luminal openings were measured. All values are presented as mean crypt length in micrometers (μm) ± standard error (SE).
*Asterisks indicate significance ($p < 0.05$).

To further characterize the changes in epithelial cell proliferation in the colon of guanylin null mice, we measured the rate of migration of BrdU- stained epithelial cells at 1, 24, or 48 hours. Following labeling with BrdU, we measured the distance from a fixed point at the base of the crypt to the farthest migrated BrdU-positive cell. This method revealed little or no change in the migration rate of ileal epithelia between heterozygous littermate and guanylin null mice (Figure 5A, Figure 6A). A change in migration rate was evident in the colon, however, as epithelia in the guanylin null mice had moved much farther from the base of the crypt by 48 hours when compared to heterozygous littermate controls (Figure 5A, Figure 6B). These data parallel the observations of cGMP levels in null mice and controls.

The presence of PCNA was used as another quantitative marker of cellular division. We determined the number of PCNA-stained cells per crypt-villus in the ileum or per crypt in the distal colon, as described in Materials and Methods. No difference was seen in the ileum (Figure 5B, Figure 7A). However, distal colonic epithelia of guanylin null mice had significantly more PCNA-stained cells per crypt than did heterozygous littermate controls (Figure 5B, Figure 7B). The number of BrdU-stained cells per crypt was similarly increased in the colon of knockout animals (3.10 ± 0.19 *versus* 3.67 ± 0.18 BrdU-stained cells, heterozygote *versus* knockout respectively, $P = 0.04$, 5 to 6 mice per genotype, total of 46 to 52 crypts examined).

TUNEL assay was used to establish rates of apoptosis by scoring the number of apoptotic bodies identified within the crypts. The apoptotic index was defined as the

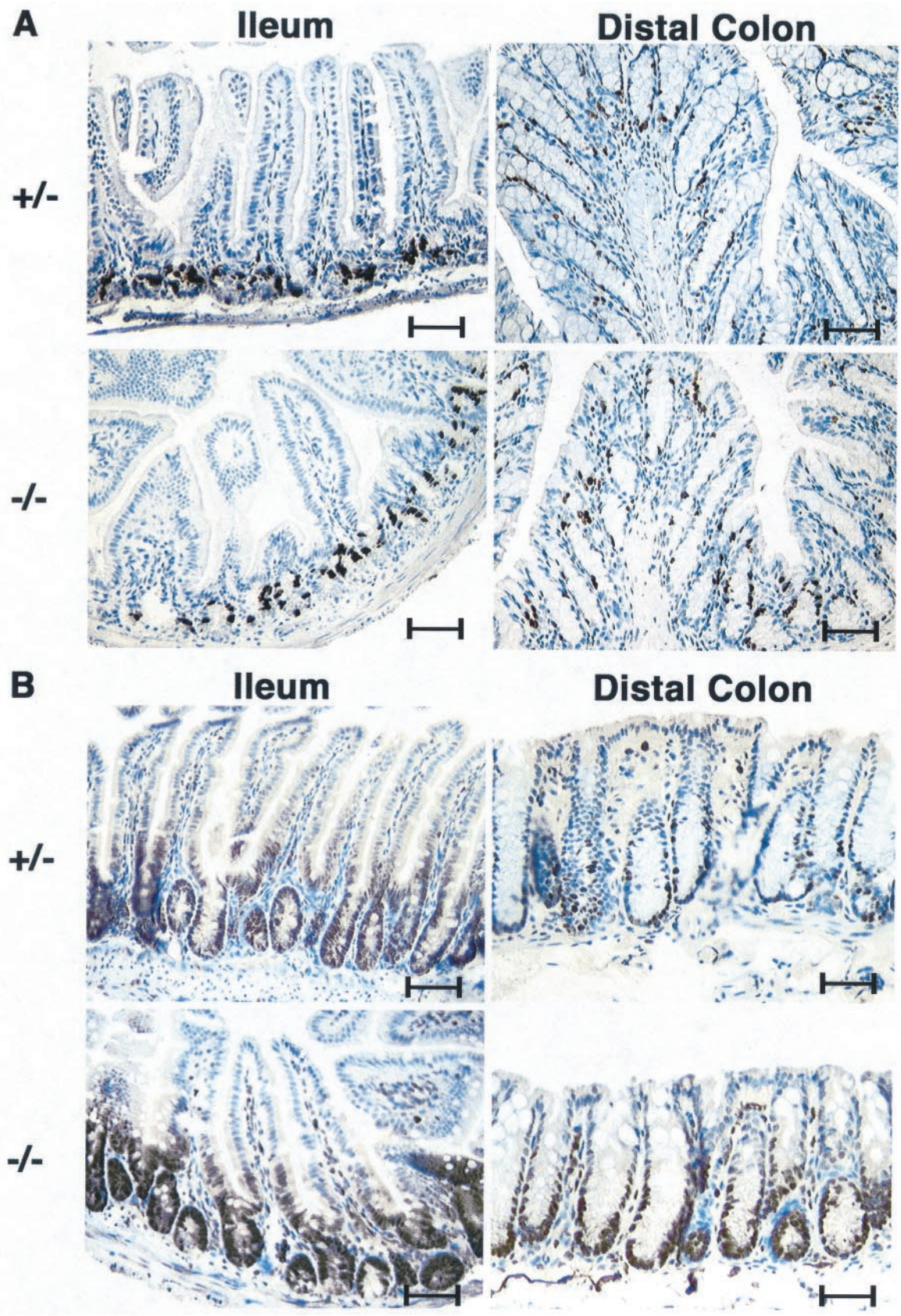

Figure 5. Immunohistochemistry. **A:** Representative sections from BrdU-injected heterozygous and guanylin null mice were visualized in ileum and distal colon at 1 hour (ileum) and 24 hours (distal colon). **B:** Representative sections from PCNA-stained ileum and distal colon of heterozygous and guanylin null mice. **Bars**, 100 μm are shown.

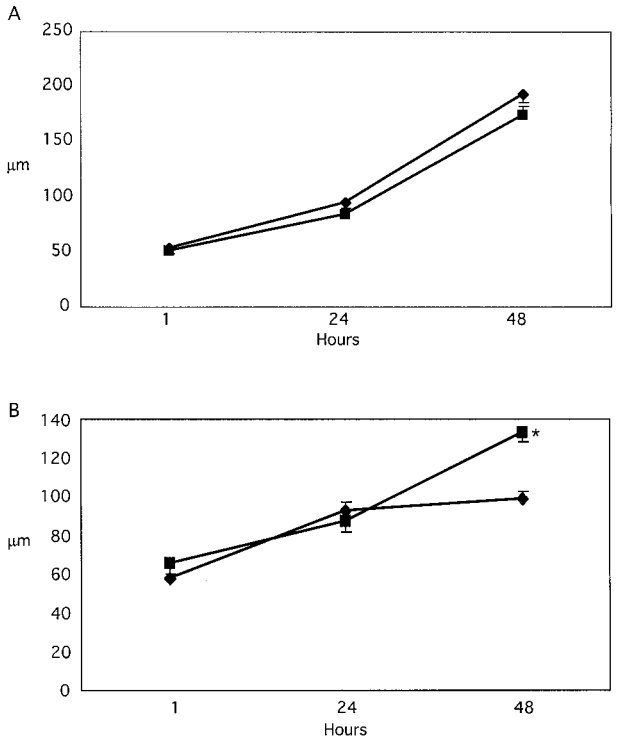

Figure 6. Epithelial cell migration. Migration of BrdU-labeled cells was quantitated as the distance (μm) from crypt to highest labeled cell in tissue harvested at 1, 24, or 48 hours after BrdU injection. **A:** Epithelial cell migration in ileum of guanylin null mice is unchanged at all time points when compared to heterozygous littermate controls. **B:** Colonic epithelia migrate farther 48 hours after BrdU injection when compared to controls. Values are presented as mean ± SE. $n = 3$ mice per genotype per each time point, > 50 crypts per mouse; *, $P < 0.001$.

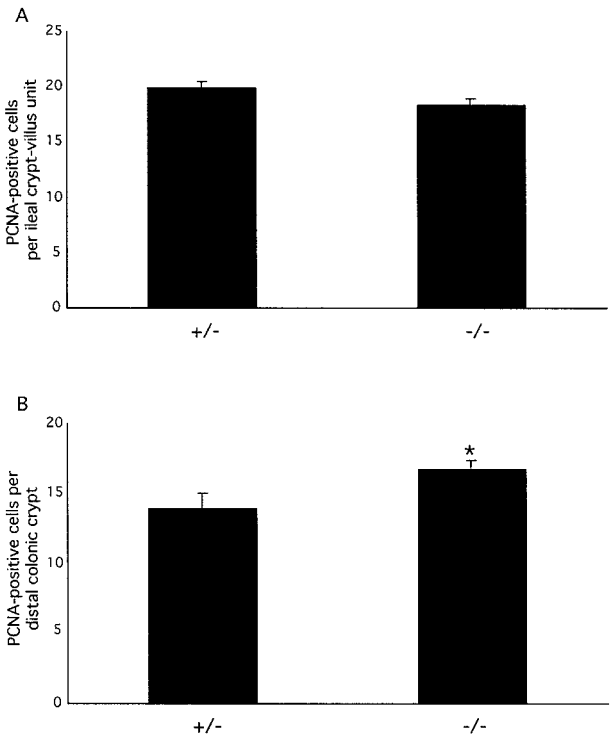

Figure 7. PCNA staining in ileum and distal colon. **A:** PCNA levels were similar in ileal epithelia of guanylin heterozygous and null mice. **B:** PCNA staining in distal colon epithelia was increased in guanylin null mice, suggesting an increased proliferation rate. Values are presented as mean ± SE. $n = 5$ to 6 mice per genotype, > 50 crypts per mouse; *, $P < 0.02$.

number of apoptotic bodies per crypt as determined by the blinded scoring and averaging of 50 to 100 crypts per sample. The apoptotic index was significantly higher in ileum compared to colon (Figure 8). However, no difference was seen in the apoptotic index between guanylin null mice and littermate controls in either location (Figure 8).

Collectively, the increased depth and number of cells in colonic crypts, the increased migration rate of colonic epithelia, and the elevated PCNA staining in colonic crypts of guanylin null mice strongly suggest an increase in the proliferation rate of epithelia of the colon.

Discussion

We have successfully inactivated the mouse guanylin gene by using a conditional deletion approach that is based on the Cre/*loxP* recombination system. Initial attempts to target the guanylin gene using a traditional neomycin resistance (neo^r) cassette to replace much of the guanylin coding sequence were unsuccessful. This approach resulted in the permanent presence of this selectable neo^r marker in the mouse genome. Despite successful generation of targeted ES cells, repeated blastocyst injections with three different ES cell strains yielded few chimeras and none gave germline transmission of the targeted guanylin allele. We hypothesized several explanations for these difficulties including a le-

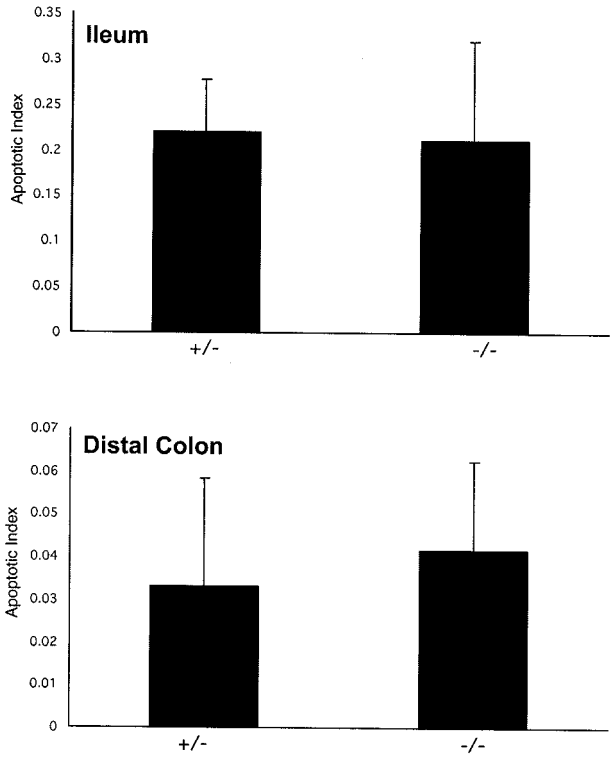

Figure 8. TUNEL assays demonstrated a similar apoptotic index in guanylin null mice and littermate controls. Apoptotic index is derived by counting the number of apoptotic bodies with characteristic nuclear location per crypt.

thal result from haploinsufficiency of the guanylin gene and the more likely explanation of the neo^r replacement cassette having a deleterious influence on nearby gene(s). There is precedent for the promoter of the neo^r selection cassette influencing expression of surrounding genes.[27] Therefore, we used the Cre/*loxP* system to allow for inactivation of guanylin in a temporal and tissue-specific manner, eg, if required to circumvent a fetal-lethal phenotype, as well as to allow for removal of the selection cassette and any difficulties it might represent.

Loss of guanylin activity did not cause severe phenotypic changes and these animals have remained healthy to at least 6 months of age. We noted few unusual deaths of adult guanylin null mice. Similarly, when raised on a standard chow diet, guanylin null mice gained weight normally and, unlike CFTR null mice, they do not demonstrate signs of intestinal obstruction,[28] presumably because there are other compensatory mechanisms in this portion of the CFTR-mediated secretory pathway. As part of a separate study, we are currently investigating the changes in colonic sodium and chloride flux and the response to secretagogues as a result of targeted deletion of the guanylin gene.

Histological examination revealed no gross changes in crypt-villus morphology or cell-type representation. However, closer examination revealed a significant decrease in cGMP levels in the colonic but not ileal mucosa of guanylin null mice. Uroguanylin levels are very high throughout the small intestine, but not the colon, and we speculate that it is the presence of uroguanylin and its subsequent activation of GC-C in the ileum that results in sustained levels of cGMP in this intestinal segment.

Changes in the level of cGMP in intestinal epithelia could be expected to influence the rate of epithelial cell proliferation.[25] We therefore used a number of different assays to determine the rate of cell proliferation in intestinal mucosa of guanylin null mice. The increase in colonic crypt depth, crypt cell number, PCNA staining, and cell migration all indicated that there was a significant increase in the rate of cell division in the colonic crypts of guanylin null mice. These data strongly support a role for guanylin in epithelial cell proliferation in the large intestine and are consistent with cGMP as a signaling molecule that is central to this process. Although the mechanism through which cGMP influences proliferation is unclear, there is substantial evidence to suggests that it regulates the rate of cell division.[25,29] Consistent loss of guanylin in mouse and human adenomatous tissue and its absence in the vast majority of intestinal cell culture lines suggest selective pressure against its presence in rapidly proliferating, transformed epithelia.[10,11,30] Guanylin and uroguanylin are located in chromosomal regions that harbor modifiers of intestinal adenoma formation susceptibility.[10,13] In addition, a recent study in human colon carcinoma cell lines indicates that the guanylin ligand family may be cytostatic, causing a slowing of cell cycle progression in a cGMP-dependent manner.[25] Collectively, these reports and the data presented here suggest that guanylin signaling has an antiproliferative effect on normal intestinal epithelia and that loss of guanylin and subsequent decreases in intracellular cGMP remove this cytostatic block and allow increased cell division. As suggested by Pitari et al,[25] these data also imply that the guanylin ligand family may play a role in regulating the transition between intestinal stem cell proliferation and differentiation into mature enterocytes. Additionally, they support a potential role for these ligands as cytostatic agents in the prevention or treatment of colorectal cancer.

There are conflicting data regarding the role of guanylin, uroguanylin, and GC-C as mediators of apoptosis. For example, cGMP is reduced in intestinal cancers due to increased cGMP-hydrolyzing phosphodiesterase activity and use of cGMP-specific phosphodiestase inhibitors in combination with guanylin causes apoptosis in transformed colonic cell lines.[31] Uroguanylin was shown to elicit profound apoptosis in human cancer cell lines.[29] However, other *in vitro* studies demonstrate no pro-apoptotic effect of STa or uroguanylin.[25] Similarly, measurement of the apoptotic index in intestinal epithelia of guanylin null mice showed no change in the number of apoptotic cells when compared to heterozygous littermates. Experimental variability that is inherent in this index prevents us from knowing whether a small increase in apoptosis is present and counterbalances the observed increase in proliferation to maintain a steady state.

Several other genes in the guanylin-signaling pathway have also been targeted. CFTR null mice exhibit a phenotype that is very similar to the guanylin null mice with respect to epithelial proliferation.[32] CFTR inactivation results in increased epithelial cell proliferation in the small intestine, a tissue where we speculate that uroguanylin compensates for the loss of guanylin and thereby diminishes the effect of guanylin loss. Data concerning the effect of loss of GC-C in mouse intestinal epithelia with regard to proliferation and apoptosis have not been reported.[33,34] Although the only known receptor for guanylin is GC-C, the existence of other receptors is strongly indicated by multiple data sets.[35,36] If the phenotype of the guanylin null mouse is mediated by GC-C, then we would predict a similar phenotype in the GC-C null mouse. The possibility remains, however, that the changes in epithelial cell proliferation and the decrease in intracellular cGMP levels are not connected *via* GC-C. Future experiments are planned to address these questions.

Acknowledgments

We thank Pam Groen, Lisa Artmeier, and Alicia Emley for their assistance.

References

1. Cohen MB, Giannella RA: Enterotoxigenic Escherichia coli. Infections of the Gastrointestinal Tract, ed 2. Edited by Blaser MJ, Smith PD, Ravdin JI, Greenberg HB. New York, Raven Press, 2002, pp 579–594
2. Currie MG, Fok KF, Kato J, Moore RJ, Hamra FK, Duffin KL, Smith CE: Guanylin: an endogenous activator of intestinal guanylate cyclase. Proc Natl Acad Sci USA 1992, 89:947–951
3. Forte LR, Currie MG: Guanylin: a peptide regulator of epithelial transport. EMBO J 1995, 9:643–650
4. Cohen MB, Witte DP, Hawkins JA, Currie MG: Immunohistochemical

localization of guanylin in the rat small intestine and colon. Biochem Biophys Res Commun 1995, 209:803–808
5. Gao Z, Yuen PS, Garbers DL: Interruption of specific guanylyl cyclase signaling pathways. Adv Second Messenger Phosphoprotein Res 1997, 31:183–190
6. Schulz S, Green CK, Yuen PS, Garbers DL: Guanylyl cyclase is a heat-stable enterotoxin receptor. Cell 1990, 63:941–948
7. Garbers DL: Guanylyl cyclase receptors and their ligands. Adv Second Messenger Phosphoprotein Res 1993, 28:91–95
8. Cuthbert AW, Hickman ME, MacVinish LJ, Evans MJ, Colledge WH, Ratcliff R, Seale PW, Humphrey PP: Chloride secretion in response to guanylin in colonic epithelial from normal and transgenic cystic fibrosis mice. Br J Pharmacol 1994, 112:31–36
9. Chao AC, de Sauvage FJ, Dong YJ, Wagner JA, Goeddel DV, Gardner P: Activation of intestinal CFTR Cl-channel by heat-stable enterotoxin and guanylin via cAMP-dependent protein kinase. EMBO J 1994, 13:1065–1072
10. Steinbrecher KA, Tuohy TM, Heppner Goss K, Scott MC, Witte DP, Groden J, Cohen MB: Expression of guanylin is down-regulated in mouse and human intestinal adenomas. Biochem Biophys Res Commun 2000, 273:225–230
11. Cohen MB, Hawkins JA, Witte DP: Guanylin mRNA expression in human intestine and colorectal adenocarcinoma. Lab Invest 1998, 78:101–108
12. Shibata H, Toyama K, Shioya H, Ito M, Hirota M, Hasegawa S, Matsumoto H, Takano H, Akiyama T, Toyoshima K, Kanamaru R, Kanegae Y, Saito I, Nakamura Y, Shiba K, Noda T: Rapid colorectal adenoma formation initiated by conditional targeting of the Apc gene. Science 1997, 278:120–123
13. Sciaky D, Jenkins NA, Gilbert DJ, Copeland NG, Sonoda G, Testa JR, Cohen MB: Mapping of guanylin to murine chromosome 4 and human chromosome 1p34–p35. Genomics 1995, 26:427–429
14. Steinbrecher KA, Mann EA, Giannella RA, Cohen MB: Increases in guanylin and uroguanylin in a mouse model of osmotic diarrhea are guanylate cyclase c-independent. Gastroenterology 2001, 121:1191–1202
15. Swenson ES, Mann EA, Jump ML, Witte DP, Giannella RA: The guanylin/STa receptor is expressed in crypts and apical epithelium throughout the mouse intestine. Biochem Biophys Res Commun 1996, 225:1009–1014
16. Whitaker TL, Witte DP, Scott MC, Cohen MB: Uroguanylin and guanylin: distinct but overlapping patterns of messenger RNA expression in mouse intestine. Gastroenterology 1997, 113:1000–1006
17. Perkins A, Goy MF, Li Z: Uroguanylin is expressed by enterochromaffin cells in the rat gastrointestinal tract. Gastroenterology 1997, 113: 1007–1014
18. Li Z, Taylor-Blake B, Light AR, Goy MF: Guanylin, an endogenous ligand for C-type guanylate cyclase, is produced by goblet cells in the rat intestine. Gastroenterology 1995, 109:1863–1875
19. Balint JP, Kosiba JL, Cohen MB: The heat-stable enterotoxin-guanylin receptor is expressed in rat hepatocytes and in a rat hepatoma (H-35) cell line. J Recept Signal Transduct Res 1997, 17:609–630
20. Stern LE, Falcone Jr RA, Kemp CJ, Braun MC, Erwin CR, Warner BW: Salivary epidermal growth factor and intestinal adaptation in male and female mice. Am J Physiol 2000, 278:G871–G877
21. Helmrath MA, VanderKolk WE, Can G, Erwin CR, Warner BW: Intestinal adaptation following massive small bowel resection in the mouse. J Am Coll Surg 1996, 183:441–449
22. Schwenk F, Baron U, Rajewsky K: A cre-transgenic mouse strain for the ubiquitous deletion of loxP-flanked gene segments including deletion in germ cells. Nucleic Acids Res 1995, 23:5080–5081
23. Whitaker TL, Steinbrecher KA, Copeland NG, Gilbert DJ, Jenkins NA, Cohen MB: The uroguanylin gene (Guca1b) is linked to guanylin (Guca2) on mouse chromosome 4. Genomics 1997, 45:348–354
24. Silberbach M, Roberts Jr CT: Natriuretic peptide signaling: molecular and cellular pathways to growth regulation. Cell Signal 2001, 13:221–231
25. Pitari GM, Di Guglielmo MD, Park J, Schulz S, Waldman SA: Guanylyl cyclase C agonists regulate progression through the cell cycle of human colon carcinoma cells. Proc Natl Acad Sci USA 2001, 98: 7846–7851
26. Chin TY, Lin YS, Chueh SH: Antiproliferative effect of nitric oxide on rat glomerular mesangial cells via inhibition of mitogen-activated protein kinase. Eur J Biochem 2001, 268:6358–6368
27. Holzenberger M, Leneuve P, Hamard G, Ducos B, Perin L, Binoux M, Le Bouc Y: A targeted partial invalidation of the insulin-like growth factor I receptor gene in mice causes a postnatal growth deficit. Endocrinology 2000, 141:2557–2566
28. Snouwaert JN, Brigman KK, Latour AM, Malouf NN, Boucher RC, Smithies O, Koller BH: An animal model for cystic fibrosis made by gene targeting. Science 1992, 257:1083–1088
29. Shailubhai K, Yu HH, Karunanandaa K, Wang JY, Eber SL, Wang Y, Joo NS, Kim HD, Miedema BW, Abbas SZ, Boddupalli SS, Currie MG, Forte LR: Uroguanylin treatment suppresses polyp formation in the Apc(Min/+) mouse and induces apoptosis in human colon adenocarcinoma cells via cyclic GMP. Cancer Res 2000, 60:5151–5157
30. Zhang L, Zhou W, Velculescu VE, Kern SE, Hruban RH, Hamilton SR, Vogelstein B, Kinzler KW: Gene expression profiles in normal and cancer cells. Science 1997, 276:1268–1272
31. Liu L, Li H, Underwood T, Lloyd M, David M, Sperl G, Pamukcu R, Thompson WJ: Cyclic gmp-dependent protein kinase activation and induction by exisulind and cp461 in colon tumor cells. J Pharmacol Exp Ther 2001, 299:583–592
32. Gallagher AM, Gottlieb RA: Proliferation, not apoptosis, alters epithelial cell migration in small intestine of CFTR null mice. Am J Physiol 2001, 281:G681–G687
33. Schulz S, Lopez MJ, Kuhn M, Garbers DL: Disruption of the guanylyl cyclase-C gene leads to a paradoxical phenotype of viable but heat-stable enterotoxin-resistant mice. J Clin Invest 1997, 100:1590–1595
34. Mann EA, Jump ML, Wu J, Yee E, Giannella RA: Mice lacking the guanylyl cyclase C receptor are resistant to STa-induced intestinal secretion. Biochem Biophys Res Commun 1997, 239:463–466
35. Carrithers SL, Hill MJ, Johnson BR, O'Hara SM, Jackson BA, Ott CE, Lorenz J, Mann EA, Giannella RA, Forte LR, Greenberg RN: Renal effects of uroguanylin and guanylin in vivo. Braz J Med Biol Res 1999, 32:1337–1344
36. Mann EA, Cohen MB, Giannella RA: Comparison of receptors for Escherichia coli heat-stable enterotoxin: novel receptor present in IEC-6 cells. Am J Physiol 1993, 264:G172–G178